Anomalous local coordination, density fluctuations, and void statistics in disordered hyperuniform many-particle ground states

Chase E. Zachary*
Department of Chemistry, Princeton University, Princeton, New Jersey 08544, USA

Salvatore Torquato†
Department of Chemistry, Department of Physics, Program in Applied and Computational Mathematics, Princeton Institute for the Science and Technology of Materials, and Princeton Center for Theoretical Science, Princeton University, Princeton, New Jersey 08544, USA

(Received 5 December 2010; published 31 May 2011)

We provide numerical constructions of one-dimensional hyperuniform many-particle distributions that exhibit unusual clustering and asymptotic local number density fluctuations growing more slowly than the volume of an observation window but faster than the surface area. Hyperuniformity, defined by vanishing infinite-wavelength local density fluctuations, provides a quantitative metric of global order within a many-particle configuration and signals the onset of an "inverted" critical point in which the direct correlation function becomes long ranged. By targeting a specified form of the structure factor at small wavenumbers ($S(k) \sim k^{\alpha}$ for $0 < \alpha < 1$) using collective density variables, we are able to tailor the form of asymptotic local density fluctuations while simultaneously measuring the effect of imposing weak and strong constraints on the available degrees of freedom within the system. This procedure is equivalent to finding the (possibly disordered) classical ground state of an interacting many-particle system with up to four-body interactions. Even in one dimension, the long-range effective interactions induce clustering and nontrivial phase transitions in the resulting ground-state configurations. We provide an analytical connection between the fraction of constrained degrees of freedom within the system and the disorder-order phase transition for a class of target structure factors by examining the realizability of the constrained contribution to the pair correlation function. Our results explicitly demonstrate that disordered hyperuniform many-particle ground states, and therefore also point distributions, with substantial clustering can be constructed. We directly relate the local coordination structure of our point patterns to the distribution of the void space external to the particles, and we provide a scaling argument for the configurational entropy (analogous to spin-frustated system) of the disordered ground states. By emphasizing the intimate connection between geometrical constraints on the particle distribution and structural regularity, our work has direct implications for higher-dimensional systems, including an understanding of the appearance of hyperuniformity and quasi-long-range pair correlations in maximally random strictly jammed packings of hard spheres.

DOI: 10.1103/PhysRevE.83.051133 PACS number(s): 05.20.−y, 61.20.Gy, 61.50.Ah

I. INTRODUCTION

The relationship between the local structure of a many-particle system and interparticle correlations is fundamental to condensed-matter theory. This intimate connection provides a useful image of the regularity [1] of all phases of matter, allowing researchers to track the local structure over increasing length scales approaching the global system. In practice, one measures pair correlations between distinct points in the form of the structure factor $S(k)$, which is proportional to the scattering intensity from x-ray or small-angle neutron scattering [2]. It is intuitive from such measurements that a hierarchy of structural order can be established, ranging from crystalline structures such as Bravais lattices [3] to highly disordered systems, the prototypical example of which is the ideal gas [4–7]. Unfortunately, quantitative descriptors consistent with this stratification of order are difficult to identify, and this area of research is currently open. One recently introduced order metric [8] involves the notion of hyperuniformity of point patterns, whereby infinite-wavelength local density fluctuations vanish [4,6]. This order metric explicitly indicates the degree to which density fluctuations are suppressed on large length scales.

The local structure of a hyperuniform many-particle configuration (i.e., on the order of a few nearest-neighbor distances between particles) is by definition indicative of the global arrangement of particles [4]. Also known as superhomogeneity [9], this phenomenon is fundamental to the description of all Bravais lattices, lattices with a multiparticle basis, quasicrystals, and certain disordered systems possessing pair correlation functions decaying to unity exponentially fast [6]. We emphasize that while hyperuniformity in periodic configurations is a trivial consequence of their intrinsic long-range order, the fact that disordered many-particle systems can also display this property is nonintuitive. This behavior is especially surprising since the appearance of hyperuniformity marks the onset of an "inverted" critical point in which the structure factor vanishes in the limit of small wavenumbers while the direct correlation function, defined through the Ornstein-Zernike formalism, becomes long ranged [4].

Hyperuniform systems have played a fundamental role in our understanding and design of materials, including those

*czachary@princeton.edu
†torquato@princeton.edu

with large, complete photonic band gaps [10], "stealth" materials invisible to certain frequencies of radiation [11], and prototypical glassy structures consisting of maximally random strictly jammed (MRJ) monodisperse hard spheres [12,13]. Other examples of disordered hyperuniform systems include noninteracting spin-polarized fermions [14,15], the ground state of liquid helium [16], the density fluctuations of the early Universe [17], one-component plasmas [4], and so-called g_2-invariant processes [4], in which the form of the pair correlation function is held fixed over a certain density interval. Note for *equilibrium* many-particle configurations at positive temperature, hyperuniformity implies that the isothermal compressibility vanishes; this relationship does not hold, however, for nonequilibrium systems.

Hyperuniform particle distributions possess structure factors with a small-wavenumber scaling $S(k) \sim k^{\alpha}$ for $\alpha > 0$, including the special case $\alpha = +\infty$ for periodic crystals. This behavior implies that the variance $\sigma_N^2(R)$ in the number of particles within a local observation window (here a d-dimensional sphere of radius R) increases asymptotically as [6]

$$\sigma_N^2(R) \sim \begin{cases} R^{d-1} \ln R, & \alpha = 1 \\ R^{d-\alpha}, & \alpha < 1 \\ R^{d-1}, & \alpha > 1 \end{cases} \quad (R \to +\infty). \qquad (1)$$

However, all known hyperuniform configurations to date have a scaling parameter $\alpha \geqslant 1$ [18,19], meaning that the second asymptotic regime of the number variance in (1) has never been observed in either theoretical or experimental studies. Indeed, the aforementioned MRJ packings, which are *maximally* disordered among all jammed sphere packings with diverging elastic moduli, possess a small-wavenumber scaling $\alpha = 1$, and this observation has provoked the question of whether this value corresponds to a *minimal* scaling among all hyperuniform point patterns. Zachary, Jiao, and Torquato have provided strong arguments that this claim is indeed true for strictly jammed hard-particle packings [13], but it is unclear whether general point patterns must also possess exponents $\alpha \geqslant 1$. Here we provide for the first time constructions of "anomalous" disordered hyperuniform many-particle (zero-temperature) ground states for which $\alpha < 1$, demonstrating the diversity of possible structures within of this class of systems.

Our approach involves placing explicit constraints on the so-called collective coordinates associated with a point distribution, which are defined by a Fourier transform of the local density variable (discussed in Sec. II below) [18,20,21]. Controls on collective coordinates have been previously used in the development of novel stealth materials [11] and in the identification of unusual disordered classical ground states for certain classes of pair potentials [22]. In general, the problem of constraining collective coordinates can be viewed as the determination of the ground state of a many-particle system, possibly with up to four-body interactions [18]; duality relations, which relate the energy per particle of a many-body potential in real space to the corresponding energy of the dual (Fourier-transformed) potential, can be used to examine analytically the ground-state structures and energies [23]. Importantly, since collective coordinates directly probe the configuration space associated with the two-particle information of the structure factor, they are ideally suited to the construction of hyperuniform point patterns. Formally, we numerically construct a configuration of particles whose spatial distribution is consistent with a targeted form of the structure factor at small wavenumbers. By constraining a certain number of degrees of freedom in the system, we "fix" the positions of a known fraction of the total number of particles based on the locations of the remaining particles and the implicit constraints imposed by the targeted form of $S(k)$. By varying the fraction of constrained degrees of freedom within the system, we are able to explore directly the relationship between hyperuniformity and internal structural constraints of a many-particle configuration, allowing us to interpolate between the "disordered" and "ordered" regimes of hyperuniformity. We note that this same technology of placing constraints on collective coordinates has recently been used in the design of novel hyperuniform disordered materials with complete photonic band gaps [10], which have recently been fabricated in the laboratory [24].

In order to elucidate the connection between the local coordination structure and pair correlations for our anomalous hyperuniform ground states, we have investigated the distribution of the available *void space* external to the particles. Prior work on MRJ packings of binary hard disks has shown that the appearance of hyperuniformity in a many-particle system is related to the underlying distribution of the local voids between particles [13]; in this sense, the void space is more fundamental to the local structure than the particles themselves. Strong arguments have also been put forth to support the claim that exponential values α less than unity in the small-wavenumber region of the structure factor indicate the presence of larger interparticle voids with higher frequency, thereby deregularizing the microstructure while maintaining hyperuniformity [13]. This behavior is notable since it is not obvious that hyperuniformity can be consistent with a highly clustered microstructure; see Fig. 1. Here we provide further evidence to link rigorously the void space and the local coordination structure of a point pattern, and we highlight the differences in the void space distribution for "regular" and "anomalous" hyperuniform systems. Since we can directly control the fraction of constrained degrees of freedom

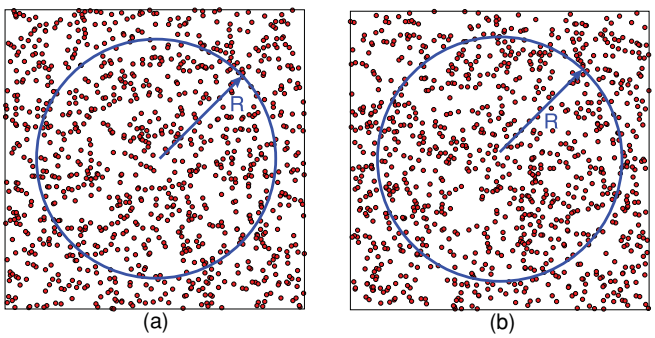

FIG. 1. (Color online) Numerically generated configurations of particles in two dimensions with a circular local observation window of radius R. Both configurations exhibit strong local clustering of points and possess a highly irregular local structure; however, configuration (a) is hyperuniform while (b) is not. The hyperuniform point pattern was generated with the same methodology outlined in Sec. III of the text.

via collective coordinates, our results have implications for understanding how the void space distribution is affected by increased constraints on the many-particle configuration. Indeed, our work directly supports the fundamental role of the void space in the microstructure and reinforces the relationship between constraints on the local structure and the aforementioned observed minimal scaling $\alpha = 1$ found in $S(k)$ for MRJ hard-sphere packings, which are glassy nonequilibrium structures.

Our major results are summarized as follows:

(i) Disordered hyperuniform many-particle ground states can, counterintuitively, exhibit a substantial degree of clustering in the absence of a large number of constraints on the particle distribution (Secs. IV and V).

(ii) The order-disorder phase transition in ground states that occurs on increasing the fraction of constrained degrees of freedom is related to the *realizability* of the constrained contribution to the pair correlation function $g_2(r)$ (defined below) (Sec. IV).

(iii) Hyperuniform particle distributions with anomalous asymptotic local density fluctuations (i.e., slower than the volume but faster than the surface area of an observation window) can be constructed, and these fluctuations are intimately related to the distribution of *void sizes* external to the particles (Sec. V).

(iv) With few constrained degrees of freedom (e.g., a perturbation from an ideal gas), the entropy (configurational degeneracy) of the disordered ground states decreases linearly with the number of constraints imposed on the particle distribution (Sec. V).

Section II provides a brief overview of the important ideas related to point processes, collective coordinates, and hyperuniformity. We apply these concepts in Sec. III to discuss how control over collective coordinates can be used to numerically generate configurations of hyperuniform point patterns, including those with anomalous asymptotic local density fluctuations, to a high numerical precision. Section IV explores how increasing the fraction of constrained degrees of freedom within hyperuniform systems affects the observed pair correlations and, therefore, the local coordination structure. In Sec. V we provide explicit calculations for the void statistics of our hyperuniform point patterns under weak and strong constraints, and we draw explicit connections among the regularity of the local structure, the exponential form of the small-wavenumber region of the structure factor, and the distribution of the local voids. Concluding remarks are given in Sec. VI.

II. STOCHASTIC POINT PATTERNS, COLLECTIVE COORDINATES, AND HYPERUNIFORMITY

We consider many-particle configurations to be realizations of stochastic point processes in some subset of Euclidean space $\mathbb{R}^d$. A (finite) *stochastic point pattern* is formally defined as a distribution of N points $\{\mathbf{r}^N\}$ in some compact space $\mathcal{V}$ of volume (Lebesgue measure) V. We consider the case where the distribution is statistically homogeneous with periodic boundary conditions on $\mathcal{V}$; the thermodynamic limit $N, V \to +\infty$ with $\rho = N/V =$ constant can be taken appropriately to extend the point pattern to Euclidean space $\mathbb{R}^d$. The statistics of the process are determined by an N-particle probability density function $P_N(\mathbf{r}^N)$, which need not be a Gibbs measure. Equivalently, one can specify the countable set of *generic* n-particle probability density functions $\rho_n(\mathbf{r}^n)$, defined by

$$\rho_n(\mathbf{r}^n) = \frac{N!}{(N-n)!} \int P_N(\mathbf{r}^n, \mathbf{r}^{N-n})\, d\mathbf{r}^{N-n}. \tag{2}$$

The function ρ_n is therefore the probability density associated with finding a subset of *any* n particles within volume elements $d\mathbf{r}^n$. Note that for statistically homogeneous point patterns $\rho_1 = \rho$. Related to the generic n-particle probability density function is the n-particle correlation function $g_n(\mathbf{r}^n)$, defined by

$$\rho^n g_n(\mathbf{r}^n) = \rho_n(\mathbf{r}^n). \tag{3}$$

Of particular importance is the *pair correlation function* $g_2(\mathbf{r})$, which can be made integrable by subtracting its long-range value of unity to give the *total correlation function* $h(\mathbf{r}) = g_2(\mathbf{r}) - 1$. A Fourier representation of $g_2(\mathbf{r})$ is given by the *structure factor* $S(\mathbf{k})$, defined by

$$S(\mathbf{k}) = 1 + \rho \hat{h}(\mathbf{k}), \tag{4}$$

where we utilize the following convention for the Fourier transform:

$$\hat{f}(\mathbf{k}) = \int_{\mathbb{R}^d} \exp(-i\mathbf{k}\cdot\mathbf{r}) f(\mathbf{r})\, d\mathbf{r}. \tag{5}$$

Corresponding to any *single* configuration of points $\{\mathbf{r}^N\}$ is a local density variable

$$\rho(\mathbf{r}) = \sum_{j=1}^{N} \delta(\mathbf{r} - \mathbf{r}_j), \tag{6}$$

where δ denotes the Dirac δ function. The ensemble average of this local density with respect to the statistics of the point process is

$$\langle \rho(\mathbf{r}) \rangle = \rho, \tag{7}$$

and the autocorrelation function is given by

$$\langle \rho(\mathbf{r}_1)\rho(\mathbf{r}_2) \rangle = \rho\delta(\mathbf{r}) + \rho^2 g_2(\mathbf{r}) \tag{8}$$

with $\mathbf{r} = \mathbf{r}_1 - \mathbf{r}_2$. Note from Eq. (8) that the autocorrelation function contains two contributions: a δ function corresponding to the self-correlation of a point in the process and the pair correlation function between two distinct particles. The self-correlation contribution is *independent* of the distribution of particles in the system and arises for all correlated and uncorrelated point patterns.

For statistically homogeneous point patterns subject to periodic boundary conditions, it is standard and computationally convenient to assume ergodicity and equate ensemble averages with volume averages over the unit cell. This assumption is expected to be valid in the thermodynamic limit. One can show that the volume-averaged local density and autocorrelation function are

$$\overline{\rho(\mathbf{r})} = \rho \tag{9}$$

$$\overline{\rho(\mathbf{x}+\mathbf{r})\rho(\mathbf{x})} = \rho\delta(\mathbf{r}) + \frac{1}{V} \sum_{j \neq \ell = 1}^{N} \delta(\mathbf{r} - \mathbf{r}_{j\ell}), \tag{10}$$

where $\mathbf{r}_{j\ell} = \mathbf{r}_j - \mathbf{r}_\ell$. Equation (10) suggests the following alternative definition of the pair correlation function, which is well known [25]:

$$\rho^2 g_2(\mathbf{r}) = \left\langle \frac{1}{V} \sum_{j\neq\ell=1}^{N} \delta(\mathbf{r} - \mathbf{r}_{j\ell}) \right\rangle. \tag{11}$$

Since the Dirac δ functions in Eq. (10) are by definition localized, this result has little practical utility when handling finite particle distributions. However, one can take advantage of the periodicity of the unit cell to expand the local density in a Fourier series according to

$$\rho(\mathbf{r}) = \frac{1}{V} \sum_{j=1}^{N} \sum_{\mathbf{k}} \exp[i\mathbf{k}\cdot(\mathbf{r} - \mathbf{r}_j)], \tag{12}$$

which is equivalent to a discrete (inverse) Fourier transform. The wave vectors $\mathbf{k}$ in Eq. (12) are determined by the geometry of the unit cell; if the unit cell is formed with basis vectors $\{\mathbf{e}_i\}$, then the wave vectors satisfy

$$\mathbf{k}\cdot\mathbf{e}_i = 2\pi m \tag{13}$$

for all i and for some $m \in \mathbb{Z}$. For simplicity, we will henceforth consider a d-dimensional cubic cell $[0,L]^d \subset \mathbb{R}^d$, which implies $\mathbf{k} = 2\pi\mathbf{n}/L$ for some $\mathbf{n} \in \mathbb{Z}^d$. Rewriting (12) in the form

$$\rho(\mathbf{r}) = \frac{1}{V} \sum_{\mathbf{k}} \exp(i\mathbf{k}\cdot\mathbf{r})\hat{\rho}(\mathbf{k}), \tag{14}$$

where

$$\hat{\rho}(\mathbf{k}) = \sum_{j=1}^{N} \exp(-i\mathbf{k}\cdot\mathbf{r}_j), \tag{15}$$

we observe that the local density is the discrete (inverse) Fourier transform of $\hat{\rho}$, which we call a *collective density variable*.

The identity (9) can also be obtained using the Fourier representation (12), meaning that only the mode $\mathbf{k} = \mathbf{0}$ contributes to the local density on average. However, the autocorrelation function is now of the form

$$\begin{aligned}\overline{\rho(\mathbf{x}+\mathbf{r})\rho(\mathbf{x})} &= \frac{\rho}{V} \sum_{\mathbf{k}} \exp(i\mathbf{k}\cdot\mathbf{r}) \\ &\quad + \frac{1}{V^2} \sum_{j\neq\ell} \sum_{\mathbf{k}} \exp[i\mathbf{k}\cdot(\mathbf{r} - \mathbf{r}_{j\ell})] \qquad (16)\\ &= \rho\delta(\mathbf{r}) + \frac{\rho^2}{N^2} \sum_{\mathbf{k}} \exp(i\mathbf{k}\cdot\mathbf{r})[|\hat{\rho}(\mathbf{k})|^2 - N], \qquad (17)\end{aligned}$$

which, by comparing with (8), implies [26]

$$g_2(\mathbf{r}) = \frac{1}{N^2} \sum_{\mathbf{k}} \exp(i\mathbf{k}\cdot\mathbf{r})[\langle|\hat{\rho}(\mathbf{k})|^2\rangle - N]. \tag{18}$$

The result (18) allows one to directly compute the pair correlation function from the collective density variables $\hat{\rho}$; note that the $\mathbf{k} = \mathbf{0}$ mode must be included in this calculation to ensure the correct long-range behavior $g_2(\mathbf{r}) \to 1$ as $\|\mathbf{r}\| \to +\infty$. In practice, one must truncate the wave vector summation in (18), leading to oscillatory approximations to g_2 within some threshold determined by the cut-off magnitude of the wave vectors.

Hyperuniform point patterns constitute a subclass of point processes lacking infinite-wavelength local density fluctuations [4]. Specifically, it has been shown that the variance $\sigma_N^2(R)$ in the number of points within a local spherical observation window $\mathcal{W}(R)$ of radius R and volume $v(R)$ scales asymptotically as [4]

$$\begin{aligned}\sigma_N^2(R) = \langle N(R)\rangle [&A_N(R) + B_N(R)/R \\ &+ \text{lower-order terms}],\end{aligned} \tag{19}$$

where $\langle N(R)\rangle = \rho v(R)$ is the average number of points in the observation window. The coefficients $A_N(R)$ and $B_N(R)$ in (19) are determined solely by the two-particle information of the point pattern:

$$A_N(R) = 1 + \rho \int_{\mathcal{W}(R)} h(\mathbf{r})\, d\mathbf{r} \quad (R \to +\infty) \tag{20}$$

$$B_N(R) = -\frac{\rho\Gamma(1+d/2)}{\Gamma[(d+1)/2]\Gamma(1/2)} \int_{\mathcal{W}(R)} h(\mathbf{r}) r\, d\mathbf{r}\ (R \to +\infty). \tag{21}$$

So long as $h(r) \to 0$ faster than r^{-d}, the leading-order coefficient $A_N(R)$ converges asymptotically as $A_N(R) = A_N \equiv \lim_{\|\mathbf{k}\|\to 0} S(\mathbf{k})$ [27]. By definition, a hyperuniform point pattern possesses a number variance growing slower than the volume $v(R)$ of the observation window (equivalently, the mean number of points $\langle N(R)\rangle$), implying that $A_N = 0$ and infinite-wavelength density fluctuations vanish.

The most common examples, including all Bravais lattices, periodic non-Bravais lattices, quasicrystals possessing Bragg peaks, and certain disordered point patterns with pair correlation functions decaying to unity exponentially fast, of hyperuniform point patterns possess constant number variance coefficients $B_N(R) = B_N$ [4]. This behavior implies that the isotropic structure factor $S(k)$ possesses a small-wavenumber scaling Dk^α with $\alpha \geqslant 2$, including the special case $\alpha = +\infty$ for periodic structures. However, it is also possible to find hyperuniform point patterns for which $0 < \alpha < 2$, in which case $C_1 \leqslant B_N(R) < C_2 R$ as $R \to +\infty$ for some constants C_1 and C_2. The most well-known examples of these types of "anomalous" local density fluctuations occur when $S(k) \sim k$ as $k \to 0$, in which case $B_N(R) = A_1 \ln(R) + A_2$ with A_1 and A_2 constant. This situation has been well-characterized in three-dimensional maximally random jammed packings of hard spheres [12], the ground states of liquid helium [16], and noninteracting spin-polarized fermion ground states [14]. However, examples where $\alpha < 1$ have heretofore not appeared in the literature.

III. COLLECTIVE COORDINATE CONSTRUCTION OF HYPERUNIFORM POINT PATTERNS

One goal of this work is to construct examples of hyperuniform point patterns possessing the aforementioned "anomalous" asymptotic local density fluctuations, meaning that the number variance grows slower than the volume of an observation window but faster than the surface area. Collective density variables provide an attractive means to control the

small-wavenumber region of the structure factor $S(\mathbf{k})$, thereby allowing us to construct a hyperuniform point pattern with targeted local density fluctuations. Specifically, we define an objective function Φ according to

$$\Phi(\mathbf{r}^N) = \sum_{\mathbf{k}\in\mathcal{Q}} [S(\mathbf{k};\mathbf{r}^N) - S_0(\mathbf{k})]^2, \tag{22}$$

where $S_0(\mathbf{k})$ is the targeted form of the structure factor and $\mathcal{Q}$ denotes some finite subset of wave vectors $\mathbf{k}$. The structure factor is determined using collective density variables; specifically,

$$S(\mathbf{k};\mathbf{r}^N) = \frac{|\hat{\rho}(\mathbf{k})|^2}{N} \quad (\mathbf{k}\neq\mathbf{0}), \tag{23}$$

where $\hat{\rho}(\mathbf{k})$, implicitly a function of the particle positions $\mathbf{r}^N$, is defined by (15). The zero-wave vector is excluded from (23) since it provides an $\mathcal{O}(N)$ contribution to the structure factor, corresponding to a δ function in the thermodynamic limit from the long-range behavior of g_2. By expanding (22), one can show that our minimization problem corresponds to finding the classical ground state of a many-particle system with up to four-body interactions [18]

$$\Phi(\mathbf{r}^N) = \sum_{i\neq j\neq \ell\neq m} v_4(\mathbf{r}_i,\mathbf{r}_j,\mathbf{r}_\ell,\mathbf{r}_m) + \sum_{i\neq j\neq \ell} v_3(\mathbf{r}_i,\mathbf{r}_j,\mathbf{r}_\ell) + \sum_{i\neq j} v_2(\mathbf{r}_i,\mathbf{r}_j) + v_0, \tag{24}$$

where

$$v_4(\mathbf{r}_i,\mathbf{r}_j,\mathbf{r}_\ell,\mathbf{r}_m) = \frac{1}{N^2}\sum_{\mathbf{k}\in\mathcal{Q}} \cos(\mathbf{k}\cdot\mathbf{r}_{ij})\cos(\mathbf{k}\cdot\mathbf{r}_{\ell m}) \tag{25}$$

$$v_3(\mathbf{r}_i,\mathbf{r}_j,\mathbf{r}_\ell) = \frac{4}{N^2}\sum_{\mathbf{k}\in\mathcal{Q}} \cos(\mathbf{k}\cdot\mathbf{r}_{ij})\cos(\mathbf{k}\cdot\mathbf{r}_{i\ell}) \tag{26}$$

$$v_2(\mathbf{r}_i,\mathbf{r}_j) = \frac{2}{N}\sum_{\mathbf{k}\in\mathcal{Q}} \cos(\mathbf{k}\cdot\mathbf{r}_{ij})[1 - S_0(\mathbf{k})] \tag{27}$$

$$v_0 = \sum_{\mathbf{k}\in\mathcal{Q}} [S_0(\mathbf{k}) - 1]^2. \tag{28}$$

The set $\mathcal{Q}$ in (22) is chosen to contain all wave vectors, excluding the zero mode, with norm less than some upper bound K. This construction allows us to target specifically the small-wavenumber region of the structure factor, which controls the asymptotic local density fluctuations. The target function S_0 is chosen with the form

$$S_0(\mathbf{k}) = D\|\mathbf{k}\|^\alpha \quad \text{for all} \quad \mathbf{k}\in\mathcal{Q}. \tag{29}$$

In order for the target function to correspond to a realizable point pattern, it is necessary that $D \geqslant 0$ to enforce positivity of the structure factor. The parameter α determines the asymptotic behaviors of the pair correlation function and the number variance [cf. (1)]. Previous work [18] has considered the array $\alpha = 1,2,4,6,8$, and 10 in dimensions $d = 2$ and 3. It has recently been conjectured that $\alpha = 1$ corresponds to the *minimal* exponent consistent with the constraints of saturation and strict jamming in sphere packings [13]; however, systems for which $\alpha < 1$ have not been reported in the literature, and their statistical properties are unknown. The objective function (22) is minimized to within 10^{-17} of its global minimum using the MINOP algorithm [28,29], which has several computational advantages for this type of investigation as previously reported in the literature [18]. MINOP applies a dogleg strategy that uses a gradient direction when one is far from the minimum, a quasi-Newton direction when one is close, and a linear combination of the two when one is at intermediate distances from the minimum.

It is important for this study to verify that the constructed ground-state point patterns are indeed hyperuniform with the correct targeted asymptotic local density fluctuations. This criterion requires high resolution of the small-wavenumber region of the structure factor. Specifically, the smallest observable wavenumber magnitude in the collective coordinates representation (in a d-dimensional cubic unit cell) is $k_{\min} = 2\pi/L = 2\pi\rho^{1/d}/N^{1/d}$, where L is the box length, N is the number of particles, and ρ is the number density. To ensure hyperuniformity, we therefore require that $\lim_{N\to+\infty} S(k_{\min}) = 0$, where the limit is taken at constant density.

Since any simulation necessarily requires choosing N finite, it is essential to select a value of N sufficiently large to enforce both hyperuniformity and the desired form of the structure factor near the origin. Unfortunately, the $\mathcal{O}(N^{-1/d})$ scaling of $k_{\min}$ makes obtaining such resolution increasingly difficult in higher dimensions. Our interest is in verifying the existence of anomalous hyperuniform point patterns and understanding their statistical properties, and we therefore limit our studies to one dimension, where the scaling is most favorable, with $N = 2000$ particles. It should be appreciated, however, that hyperuniform point patterns with logarithmically-growing asymptotic density fluctuations are known in arbitrarily high dimensions [14]. Importantly, since our minimization procedure is equivalent to finding the classical ground state of a long-range interaction with up to four-body potentials and can be used in principle to construct hyperuniform point patterns in any dimension, nontrivial phase behaviors can still be observed [30], and we are therefore able to extend our conclusions to higher-dimensional structures.

IV. COLLECTIVE COORDINATES AND REALIZABILITY OF POINT PATTERNS

For a general d-dimensional point pattern of N particles, there are dN translational degrees of freedom in the absence of constraints on the system. One must therefore choose a set of wave vectors $\mathcal{Q}$ for the objective function (22) containing only a fraction χ of these degrees of freedom. In one dimension there are $2M(K) = \text{floor}(KL/\pi)$ wave vectors, excluding the zero mode, with magnitude less than or equal to K. Inversion invariance of the modulus of the collective density variable implies that $M(K)$ of these wave vectors can be independently constrained; we therefore define a new parameter

$$\chi = \frac{M(K)}{dN}, \tag{30}$$

which represents the fraction of independently constrained degrees of freedom from the objective function Φ.

For the case where the targeted structure factor $S_0(\mathbf{k}) = 0$ for all $\mathbf{k}\in\mathcal{Q}$, it has been previously shown [20] that increasing the parameter χ induces a greater degree of order on the particle distribution. Specifically, in one dimension the corresponding point patterns are disordered for $0 < \chi < 1/3$

and crystalline for $\chi > 1/2$ [31]; intermediate values of χ interpolate between these two regimes [32]. However, it is known that target functions of the form (29) interfere with this order-disorder phase transition; here we provide analytical results suggesting that this transition is shifted to higher values of χ for all finite α [33].

For a one-dimensional point pattern, the wave vectors are of the form $k = 2\pi m/L$ for $m \in \mathbb{Z}$, and one can write the collective density variable as

$$\hat{\rho}(m) = \sum_{j=1}^{N} \exp(-i2\pi m r_j/L). \tag{31}$$

Additionally, the total correlation function is of the form [cf. (18)]

$$h(r) = \frac{2}{N^2} \sum_{m=1}^{+\infty} \cos(2\pi m r/L)[|\hat{\rho}(2\pi m/L)|^2 - N], \tag{32}$$

which for the targeted point pattern can be decomposed as

$$h(r) = \frac{2}{N} \sum_{m=1}^{M} \cos(2\pi m r/L)[D(2\pi m/L)^{\alpha} - 1] + \frac{2}{N^2} \sum_{m=M+1}^{+\infty} \cos(2\pi m r/L)[|\hat{\rho}(2\pi m/L)|^2 - N] \tag{33}$$

$$= h_0(r; M) + h_1(r; M), \tag{34}$$

where $h_0(r; M)$ is the contribution to the total correlation function due to *constrained* wave vectors and $h_1(r; M)$ is the *unconstrained* contribution. The function h_0 can be simplified as

$$h_0(r; M) = \left(\frac{2^{\alpha+1}\pi^{\alpha} D}{N L^{\alpha}}\right) \sum_{m=1}^{M} \cos(2\pi m r/L) m^{\alpha} - \frac{2}{N} \sum_{m=1}^{M} \cos(2\pi m r/L) \tag{35}$$

$$= C(\alpha, D) \sum_{m=1}^{M} \cos(2\pi m r/L) m^{\alpha} - (2/N) \times \cos[(M+1)\pi r/L] \csc(\pi r/L) \sin(M\pi r/L), \tag{36}$$

where

$$C(\alpha, D) = \frac{2^{\alpha+1}\pi^{\alpha} D}{N L^{\alpha}} \tag{37}$$

is a parameter-dependent constant. The global minimum of $h_0(r; M)$ occurs at $r = 0$, corresponding to

$$h_0(0; M) = C(\alpha, D) \sum_{m=1}^{M} m^{\alpha} - (2M/N) \tag{38}$$

$$= C(\alpha, D) H^{(-\alpha)}(M) - (2M/N), \tag{39}$$

where

$$H^{(\alpha)}(n) = \sum_{m=1}^{n} m^{-\alpha} \tag{40}$$

is the *harmonic number* of order α.

The negative contribution to $h_0(0; M)$ in (39) suggests that there may be an upper threshold M^* beyond which $h_0(0; M) + 1 < 0$. For any values of M in this region, the constrained contribution h_0 to the total correlation function of the point pattern is no longer in itself *realizable* as a point process. The realizability problem in classical statistical mechanics [34] and the associated N-representability problem in quantum statistics [35] are notoriously difficult and unsolved problems in physics that ask under what sufficient and necessary conditions a reduced two-particle correlation function can be expressed as the integral over a full N-particle probability density. In the classical case, one can consider specifying a pair correlation function g_2 and attempting to construct a corresponding point process. Known necessary realizability conditions on g_2 include

$$g_2(\mathbf{r}) \geqslant 0 \quad \text{for all} \quad \mathbf{r} \tag{41}$$

$$S(\mathbf{k}) \geqslant 0 \quad \text{for all} \quad \mathbf{k} \tag{42}$$

along with the somewhat weaker Yamada condition

$$\sigma_N^2(R) \geqslant \theta(1-\theta) \tag{43}$$

on the fractional part θ of the average number of particles in an observation window [36]. The Yamada condition appears easy to satisfy in all but relatively low dimensions [34]. The determination of other realizability conditions on g_2 is an open problem [37].

Figures 2 and 3 compare the pair correlation functions and the constrained contributions $h_0(r) + 1$ for numerically constructed point patterns (using the methodology of Sec. III) with small-wavenumber exponents $\alpha = 0.5, 1.0$, and 2.0 and $\chi = 0.1$ and 0.35. For $\chi = 0.1$, corresponding to a small fraction of constrained degrees of freedom, the constrained contribution $h_0(r) + 1$ places only moderate constraints on the local structure of the system, primarily controlling oscillations in g_2 beyond approximately five nearest-neighbor distances. Interestingly, the small-r behaviors of $g_2(r)$ and $h_0(r) + 1$ differ strikingly. Although the *constrained* contribution to the pair correlation function generates an effective repulsion between particle pairs, the full pair correlation function indicates a tendency for particles to cluster at short pair separations. It follows that the unconstrained contribution to the pair correlation function plays a substantial role in determining the local structure for this system.

However, the situation differs markedly on increasing the constrained degrees of freedom to $\chi = 0.35$. Figure 3 shows that the constrained contribution to g_2 almost exactly mirrors the full pair correlation function, implying that sufficiently constraining the collective density variables places a *strong* constraint on the local structure of the point pattern. It follows that the value M^* beyond which $h_0(0; M) + 1 < 0$ is an indicative precursor to the *loss of realizability* of the targeted structure factor. We have mapped the threshold value M^* (equivalently, χ^*) in Fig. 4. We emphasize that this loss of realizability is associated with negativity of the real-space pair correlation function; the structure factor itself is still positive over its entire domain. Interestingly, as the exponent α controlling the small-wavenumber region of the structure factor increases, we recover the value $\chi = 0.5$ corresponding to crystallization in the case where $S_0(\mathbf{k}) = 0$ for all $\mathbf{k} \in \mathcal{Q}$.

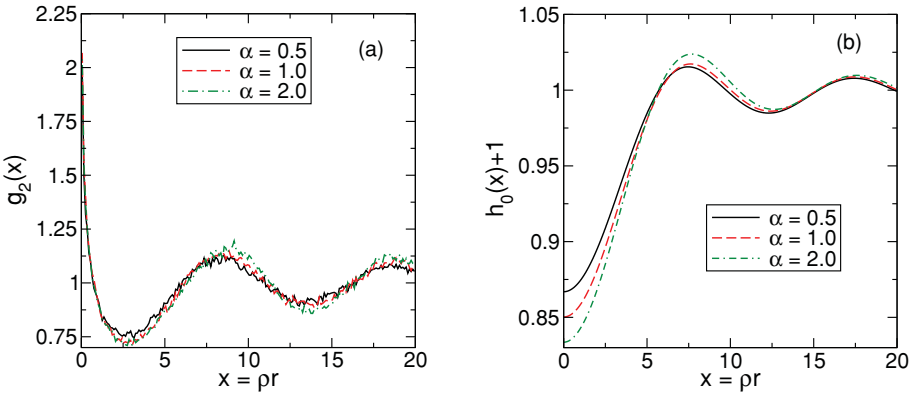

FIG. 2. (Color online) (a) Pair correlation function g_2 for numerically constructed hyperuniform point patterns with small-wavenumber scalings Dk^α and $\chi = 0.1$. (b) Constrained contributions to the pair correlation functions.

This observation suggests that the threshold values of χ beyond which $h_0(0; M) + 1 < 0$ generalize this phase transition. In Sec. V, we provide additional arguments to support this claim.

V. VOID STATISTICS AND COORDINATION STRUCTURE

A. Exclusion probability functions

The n-particle correlation functions contain information concerning the relative locations of points within a point process, and, in principle, specifying the countably infinite set (in the thermodynamic limit) of such functions is sufficient to completely determine the point pattern. However, any finite collection of correlation functions contains only partial details of the spatial arrangements of the points, implying that there are degenerate structures with these same statistics [38]. In particular, the n-particle correlations functions do not in themselves provide direct information about the space *exterior* to the points, or the so-called *void space*. It has been shown for point patterns [13,39] (and random media [40]) that the distribution of the void space is indeed a more fundamental descriptor of the point process than the arrangements of the points themselves. Here we are interested in characterizing the relationship between asymptotic local number density fluctuations and the void space statistics; in particular, we would like to examine the constraints that the exponent α in the small-wavenumber region of the structure factor places on the distribution of the void space.

One can define two types of "exclusion" functions, both of which measure the availability of empty space surrounding points of a stochastic process. The *void exclusion probability function* $E_V(r)$ is the probability of finding a d-dimensional spherical cavity of radius r centered at an arbitrary position in $\mathbb{R}^d$. The void exclusion probability has recently been shown to play a fundamental role in the covering and quantizer problems from discrete geometry and number theory [41]. Closely related to this descriptor is the *particle exclusion probability function* $E_P(r)$, which is the probability of finding a d-dimensional sphere of radius r centered on a point of the point process but containing no other points. Figure 5 highlights the differences between these functions.

The exclusion probability functions are complementary cumulative distributions of the void and particle nearest-neighbor functions $H_V(r)$ and $H_P(r)$, respectively [39,40]. The void nearest-neighbor function is the probability density of a finding the nearest point of a point process with respect to an arbitrary location in $\mathbb{R}^d$ within a radial distance $r + dr$. The particle nearest-neighbor function is defined similarly but with respect to nearest neighbors between two points of a point process. One therefore has the following simple relationships between these sets of functions:

$$H_V(r) = -\frac{\partial E_V(r)}{\partial r} \tag{44}$$

$$H_P(r) = -\frac{\partial E_P(r)}{\partial r}. \tag{45}$$

We provide a simple mathematical relationship between the void and particle exclusion functions in Appendix A.

One can without loss of generality define the *exclusion correlation function* $\eta(r)$ according to

$$\eta(r) \equiv \frac{E_P(r)}{E_V(r)}. \tag{46}$$

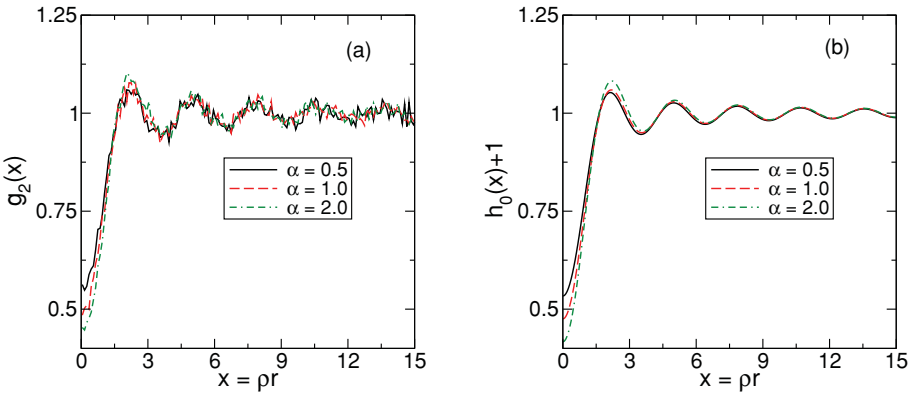

FIG. 3. (Color online) (a) Pair correlation function g_2 for numerically constructed hyperuniform point patterns with small-wavenumber scalings Dk^α and $\chi = 0.35$. (b) Constrained contributions to the pair correlation functions.

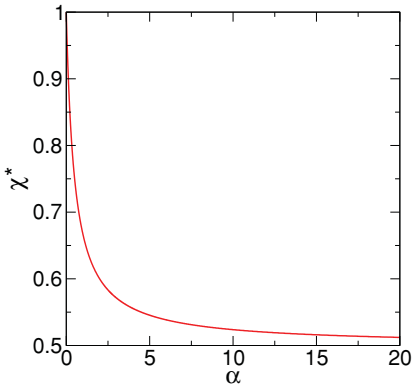

FIG. 4. (Color online) Typical threshold values $\chi^*(\alpha)$ beyond which the *constrained* contribution $h_0(r)$ to the total correlation function is no longer *realizable* as a point process. This curve corresponds to choosing $S(K) = 0.5$, where K is the magnitude of the maximally constrained wave vector. Note that as $\alpha \to +\infty$ we recover the crystallization threshold $\chi^* = 0.5$ reported in Ref. [20].

This function provides a measure of the correlations between *neighboring* points in a stochastic point pattern and is identically unity for a Poisson point process. It is interesting to note that for a system of *equilibrium* hard spheres of diameter D, the exclusion correlation function is given by [39]

$$\eta(r) = \begin{cases} [E_V(r)]^{-1} & r \leqslant D \\ [E_V(D)]^{-1} & r \geqslant D \end{cases} \tag{47}$$

which depends only on knowledge of $E_V(r)$ and is monotonically nondecreasing for all r with $\eta(0) = 1$. This result implies that the void space of an equilibrium hard-sphere system is more fundamental than the particle space [40].

Further insight into the probabilistic meanings of E_P, E_V, and η can be gained by introducing the notion of the particle space, defined to be the subset (of Lesbesgue measure zero) of $\mathbb{R}^d$ occupied by the points of the point process. The particle exclusion probability function $E_P(r)$ is then the fraction of the particle space that can be decorated by a d-dimensional sphere of radius r containing no other points of the process.

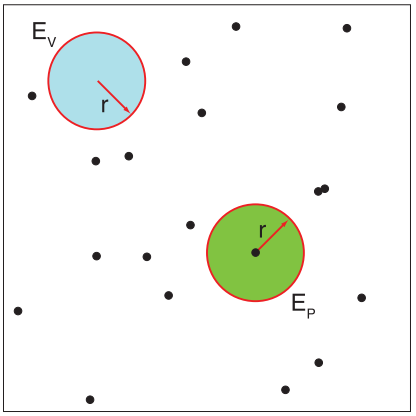

FIG. 5. (Color online) Events contributing to the void exclusion probability $E_V(r)$ (upper left) and the particle exclusion probability $E_P(r)$ (lower). The points correspond to a realization of a disordered point process.

To define the void exclusion probability $E_V(r)$, one decorates all of the points in the process by spheres of radius r and then determines the fraction of *all* space not occupied by the spheres; this value corresponds to the portion of space available to insert a cavity of radius r [41]. The exclusion correlation function $\eta(r)$ then provides a measure of the relative available space for a cavity of radius r in the particle space compared to the external void space.

Torquato and coworkers [39] have provided the following series representations for the exclusion probability functions:

$$E_V(r) = 1 + \sum_{k=1}^{+\infty} \frac{(-\rho)^k}{\Gamma(k+1)} \int g_k(\mathbf{r}^k) \prod_{j=1}^{k} m(\|\mathbf{x} - \mathbf{r}_j\|; r)\, d\mathbf{r}_j \tag{48}$$

$$E_P(r) = 1 + \sum_{k=1}^{+\infty} \frac{(-\rho)^k}{\Gamma(k+1)} \int g_{k+1}(\mathbf{r}^{k+1}) \prod_{j=2}^{k+1} \times m(\|\mathbf{r}_1 - \mathbf{r}_j\|; r)\, d\mathbf{r}_j, \tag{49}$$

where $m(r; R) = \Theta(R - r)$. Since these functions are special cases of a more general canonical n-particle correlation function [42], one can establish rigorous upper and lower bounds by truncating these series at finite order. Specifically, by writing

$$E_{V/P}(r) = \sum_{k=0}^{+\infty} E_{V/P}^{(k)}(r), \tag{50}$$

where $E_{V/P}^{(0)} \equiv 1$, we have the following hierarchy of bounds:

$$E_{V/P}(r) \leqslant \sum_{k=0}^{\ell} E_{V/P}^{(k)}(r) \quad (\ell \text{ even}) \tag{51}$$

$$E_{V/P}(r) \geqslant \sum_{k=0}^{\ell} E_{V/P}^{(k)}(r) \quad (\ell \text{ odd}), \tag{52}$$

which become sharper with increasing ℓ.

B. Local statistics of anomalous hyperuniform point patterns

We have been able to successfully construct point configurations exhibiting anomalous asymptotic local number density fluctuations. Figure 6 provides images of the structure factors for our configurations at $\chi = 0.1$ and $\chi = 0.35$. As we show, for all wave vectors within the constrained portion of the spectrum, the structure factor matches its target value within an exceedingly small numerical tolerance (on the order of 10^{-17}). In addition to the systems shown, we have also been able to reliably construct configurations with small-k exponential behaviors $\alpha \geqslant 0.25$. In order to keep the exposition clear, we have only presented results for $\alpha = 0.5$ with the disclaimer that our conclusions will apply for other point patterns with anomalous local number density fluctuations.

It is interesting to note the substantial differences in the structure factors of the systems for $\chi = 0.1$ and $\chi = 0.35$, particularly for unconstrained wave vectors. For $\chi = 0.1$, the structure factor exhibits an unusually slow decay to its asymptotic value of unity; we have fit the large-k region of the structure factor with an asymptotic fit of the form $1 + \beta/k^\gamma$ and have found a power-law decay $\gamma = 1$. This behavior is due

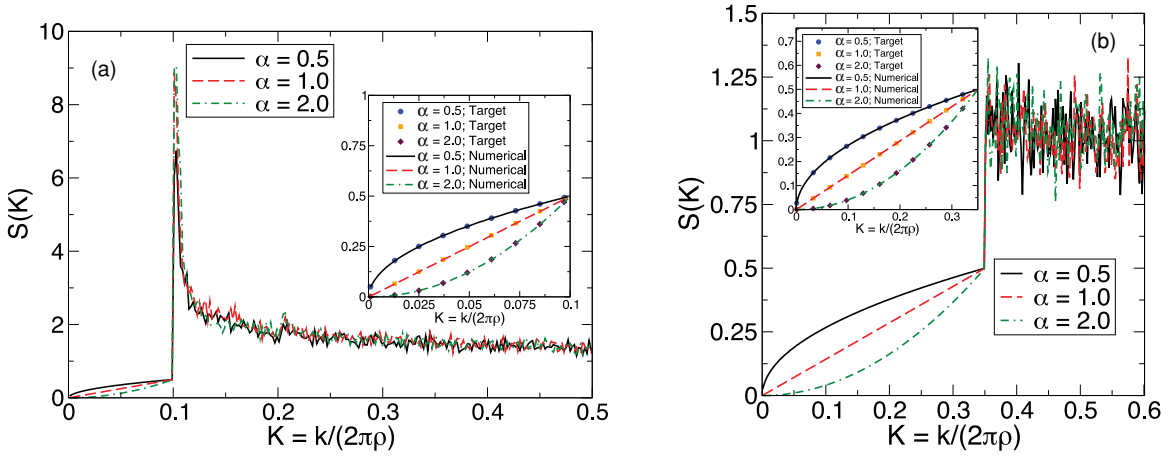

FIG. 6. (Color online) (a) Structure factor with small-k behavior Dk^{α} (inset) for numerically constructed hyperuniform point patterns with $\chi = 0.1$. (b) Structure factor with small-k behavior for $\chi = 0.35$.

to the local clustering of particles as expected from the small-r region of the pair correlation function in Fig. 2 . This effect can be directly observed in Figs. 7 and 8, which provide illustrative portions of our numerically constructed hyperuniform point patterns at $\chi = 0.1$ and $\chi = 0.35$. As has been previously reported in the literature [11,18], increasing the fraction of constrained degrees of freedom in the many-particle system has the effect of imposing greater local order in the form of an effective short-range repulsive interaction. By increasing χ from 0.1 to 0.35, the relative influence of the constrained wave vectors on the pair correlation function increases, suppressing the formation of local clusters. However, we also observe that as the exponent α controlling the small-wavenumber region of the structure factor decreases (equivalently, as anomalous local number density fluctuations appear), this effective repulsion between particles becomes noticeable weaker, manifested in the pair correlation function by larger values of $g_2(0)$. This behavior suggests that anomalous hyperuniform point patterns possess greater variability in their local structures, particularly with regard to the shapes and sizes of voids between particles.

We have verified the expected asymptotic behaviors of the number variance for our numerically constructed point patterns as shown in Fig. 9. The asymptotic scalings of these fluctuations exactly correspond to their theoretical predictions. In particular, we have provided the first example of a hyperuniform point pattern for which the asymptotic number variance grows more slowly than the volume of an observation window but faster than a logarithmic scaling. Interestingly, the local clustering of points at $\chi = 0.1$ generates strong oscillations in the number variance that persist for several nearest-neighbor distances. In contrast, these local oscillations essentially vanish after two nearest-neighbor distances at $\chi = 0.35$, reflecting the strong constraints placed on the local structure by the small-wavenumber region of the structure factor.

Our calculations for the void and particle exclusion probabilities of these systems, shown in Fig. 10, demonstrate previously unobserved statistical properties for hyperuniform point patterns. For a Poisson point pattern, one has the result that

$$E_V(r) = E_P(r) = \exp[-\rho v(r)], \tag{53}$$

implying that the exclusion correlation function $\eta(r) = 1$ for all r. This result follows from the absence of interparticle correlations for the process and the underlying Poisson probability distribution for the number of particles within an arbitrary compact set. Gabrielli and Torquato [43] have provided strong arguments to suggest that for any hyperuniform point pattern, the void exclusion probability should asymptotically decay faster than for a Poisson point process. This behavior implies that arbitrarily large cavities within the system, while not prohibited by the constraint of hyperuniformity, are expected to be significantly rare events owing to the underlying regularity of the global structure of the pattern. It is therefore not unreasonable to expect the functional form of $E_V(r)$ for the Poisson point process to provide an upper bound on the exclusion probability of any hyperuniform point pattern, and this observation is indeed rigorously true for point patterns generated from fermionic particle distributions (so-called determinantal point processes) [14]. More generally, the Poisson result will place an upper bound on E_V for any

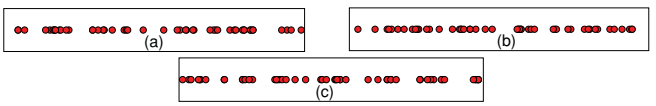

FIG. 7. (Color online) Portions of numerically constructed hyperuniform point patterns with $\chi = 0.1$ and small-k exponential scalings (a) $\alpha = 0.5$, (b) $\alpha = 1.0$, and (c) $\alpha = 2.0$. The points have been given a small but finite size for clarity.

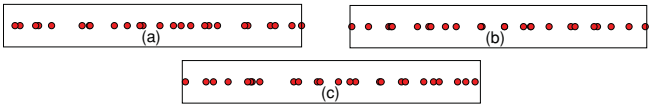

FIG. 8. (Color online) Portions of numerically constructed hyperuniform point patterns with $\chi = 0.35$ and small-k exponential scalings (a) $\alpha = 0.5$, (b) $\alpha = 1.0$, and (c) $\alpha = 2.0$. The points have been given a small but finite size for clarity.

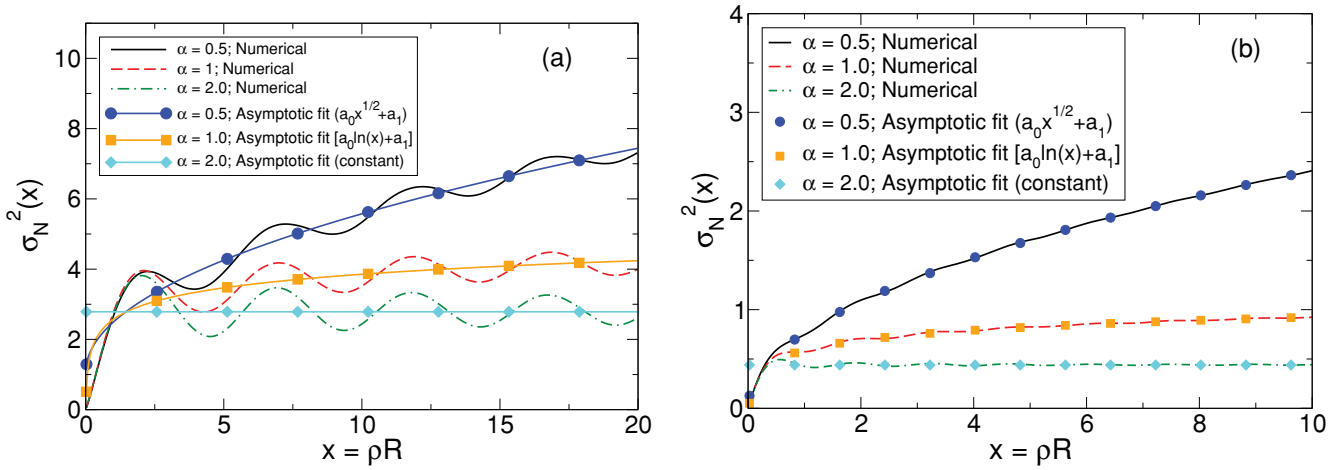

FIG. 9. (Color online) (a) Number variances $\sigma_N^2(R)$ for numerically constructed hyperuniform point patterns with $\chi = 0.1$. (b) Corresponding number variances for $\chi = 0.35$.

point pattern with n-particle correlation functions $g_n \leqslant 1$ for all n.

For $\chi = 0.1$, we observe the unusual property that $E_V(r)$ is greater than the Poisson result for all values of r that can be reliably determined from numerical simulation. It is instead the *particle* exclusion probability function that is bounded from above by the Poisson curve. To understand this discrepancy, we first note that $E_V(r)$ and $E_P(r)$ are rigorously bounded from below by [cf. (51)] [14]

$$E_V(r) \geqslant 1 - \rho v(r) \tag{54}$$
$$E_P(r) \geqslant 1 - Z(r), \tag{55}$$

where $Z(r)$ is the *cumulative coordination number*

$$Z(R) = \rho \int_{\mathbb{R}^d} \Theta(R - r) g_2(\mathbf{r})\, d\mathbf{r}. \tag{56}$$

These bounds become sharp at low density or small r. Therefore, while $E_V(r)$ is related to the geometry of a cavity within the void space, the particle exclusion probability E_P depends explicitly on the local coordination structure of the underlying point process.

To elucidate further the relationship between the local coordination structure and the void statistics, we can consider a modification of the number variance problem, whereby one measures fluctuations in the number of points within an observation window *centered on a point of the point process*. Let $N_P^{(i)}(R)$ denote this quantity; it can be represented as

$$N_P^{(i)}(R) = {\sum_{j=1}}' \Theta(R - \|\mathbf{r}_j - \mathbf{r}_i\|), \tag{57}$$

where the prime on the summation means that particle i is excluded. The average value of this random variable is

$$\left\langle N_P^{(i)}(R) \right\rangle = \rho \int_{\mathbb{R}^d} g_2(\mathbf{r}) \Theta(R - \|\mathbf{r}\|)\, d\mathbf{r} = Z(R). \tag{58}$$

The cumulative coordination number therefore measures the local number density within *the particle space*. It follows that when $Z(R) \leqslant \rho v(R)$, $\langle N_P^{(i)}(R) \rangle$, the average number of points in the particle space within an observation window of radius R, is less than or equal to $\langle N_V(R) \rangle$, the average number of points of the process within a window in the void space. This behavior then implies that the points are more greatly dispersed within the particle space, and $E_P(R) \geqslant E_V(R)$; equivalently, $\eta(R) \geqslant 1$. Note that this analysis is consistent with the lower bounds (54) and (55) on the exclusion probability functions.

Conversely, for the case where $Z(R) \geqslant \rho v(R)$, we have that $\langle N_P^{(i)}(R) \rangle \geqslant \langle N_V(R) \rangle$, which suggests that the points are more closely located within the particle space, leaving larger cavities within the void space. We therefore conclude that $E_P(R) \leqslant E_V(R)$ [$\eta(R) \leqslant 1$], and the point process should exhibit local clustering among points. These claims are also consistent with our results for the exclusion probability functions in Fig. 10, whereby we observe a transition from $\eta(R) < 1$ at $\chi = 0.1$ to $\eta(r) > 1$ for $\chi = 0.35$. Indeed, the configurations at $\chi = 0.1$ exhibit substantial clustering among points (cf. Fig. 7).

Our arguments can be extended by examining the scaling of the configurational degeneracy with the fraction of constrained degrees of freedom χ. Here we measure this degeneracy by calculating the entropy (logarithm of the degeneracy) of the system relative to an ideal gas of N particles in a volume V on the line. For the ideal gas, we coarse-grain the system by dividing the volume V into $M \gg 1$ cells such that no more than one particle occupies each cell with probability one, thereby representing the degeneracy associated with the dN translational degrees of freedom as a combinatorial occupancy problem. The size of a cell determines the length scale, meaning without loss of generality that we need only consider the regime $\rho = N/M \ll 1$. Assuming that the particles are indistinguishable, the number of configurations Ω available to the system is

$$\Omega = \frac{M!}{(M - N)!N!}. \tag{59}$$

Since the underlying distribution of particles is uniform within the cells, Boltzmann's formula for the entropy gives (with $k_B = 1$)

$$S = \ln \Omega = \ln \left[\frac{M!}{(M - N)!N!} \right], \tag{60}$$

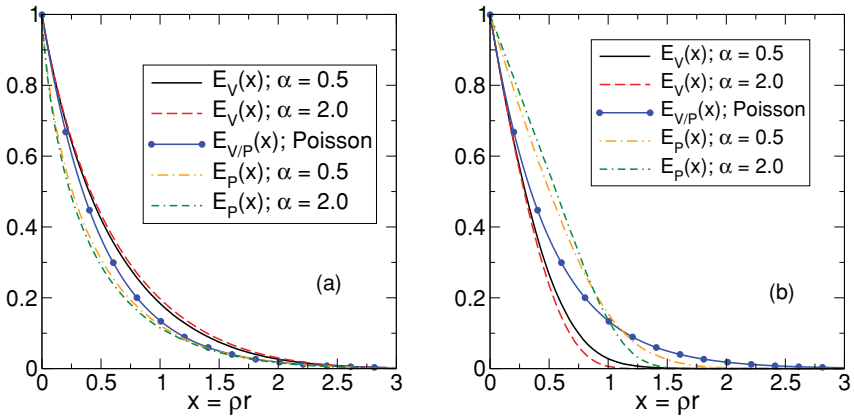

FIG. 10. (Color online) (a) Void- and particle-exclusion probabilities for the numerically constructed hyperuniform point patterns ($\chi = 0.1$) along with the reference curve for the Poisson point process. (b) Corresponding functions for $\chi = 0.35$.

which for large M and N becomes

$$S = M\ln M - M - (M-N)\ln(M-N) + (M-N) - N\ln N + N \quad (61)$$

$$= -M\ln(1-N/M) + N\ln(M/N) + N\ln(1-N/M). \quad (62)$$

Under the assumption that $N/M \ll 1$, we have the following result for the entropy per particle $\overline{S}_{\rm ideal} = S_{\rm ideal}/N$:

$$\overline{S}_{\rm ideal} = 1 - N/M + \ln(M/N) \approx 1 - \ln(\rho). \quad (63)$$

The entropy of the ideal gas is therefore large and positive as expected. For the density regime $\rho \ll 1$ that we have in mind, one can simplify further by taking $\overline{S} \approx -\ln(\rho)$, which diverges to $+\infty$ for small ρ. Note that this coarse-grained analysis is able to reproduce the expected behavior of the configurational entropy for a classical ideal gas in the continuum limit and shows that the entropy per particle is an intensive variable.

Suppose now that we constrain K degrees of freedom, where $K \ll N$. This construction correponds to making a small perturbation away from the ideal gas configuration with $N-K$ degrees of freedom still available to the many-particle system. We again divide the volume V into M cells of unit length ($N/M \ll 1$). For sufficiently small values of χ (i.e., near the ideal gas), we may assume that the length scale of the effective repulsion between particles is negligible compared to the cell size, meaning that the $N-K$ unconstrained particles may be distributed freely among the M cells. Note that the K constrained degrees of freedom are explicitly determined once these particles have been placed. The number of microstates available to the system is then

$$\Omega = \frac{M!}{(M-N+K)!(N-K)!}, \quad (64)$$

and the configurational entropy is

$$S = \ln\Omega = M\ln\left(\frac{M}{M-N+K}\right) + K\ln\left(\frac{N-K}{M-N+K}\right) + N\ln\left(\frac{M-N+K}{N-K}\right). \quad (65)$$

Defining the fraction of constrained degrees of freedom $\chi = K/N$, we may write for the entropy per particle $\overline{S} = S/N$:

$$\overline{S} = (1 - M/N - \chi)\ln(1 - N/M + \chi N/M) + (1-\chi)\ln(M/N) - (1-\chi)\ln(1-\chi), \quad (66)$$

where $\chi \ll 1$. For $N/M \ll 1$, this expression simplifies as

$$\overline{S} = 1 - \chi - (1-\chi)\ln(1-\chi) + (1-\chi)\ln(M/N) - (N/M)(1-\chi)^2. \quad (67)$$

The last term in this expression is negligible within the density regime where $\overline{S}_{\rm ideal} \approx \ln(M/N) = \ln(1/\rho)$. Since $\overline{S}_{\rm ideal}$ is large and positive compared to the first terms of this result, we have the expected scaling

$$\frac{\overline{S}}{\overline{S}_{\rm ideal}} \approx 1 - \chi, \quad (68)$$

suggesting a roughly *linear* decrease in the entropy of the system for small values of χ. Our analysis applies directly to higher-dimensional systems with the same linear scaling (68) in the relative entropy per particle, reflecting the decreasing dimension of the configurational phase space with increasing χ. We therefore provide a classical analog for particulate systems of the configurational arguments used to study the unusual residual entropy from geometrical frustration in ice and spin ice models [44]. Note that the fraction of normal modes with vanishing frequencies for the same class of disordered classical ground states has been numerically observed to scale linearly with χ [22].

By increasing the parameter α, we expect also to increase the rate at which $\overline{S} \to 0$ with respect to χ since higher values of α are associated with larger effective radii around the constrained particles. However, since we require that our configurations are hyperuniform, there are additional implicit constraints on the "unconstrained" degrees of freedom. Formally, hyperuniformity requires that the local structure of a point process approach the global structure over sufficiently short length scales, on the order of several nearest-neighbor distances. This behavior is typically associated with a highly regularized distribution of points, such as with a Bravais lattice. However, our results for E_V at $\chi = 0.1$ suggest an alternative mechanism by which hyperuniformity can be achieved in a point pattern. Specifically, the fact that $\eta(r) < 1$ is consistent with local clusters of particles that are *globally* regularized by an increased probability of finding sufficiently large voids to separate them. In this case, the appearance of these large voids external to the particle space is apparently essential to

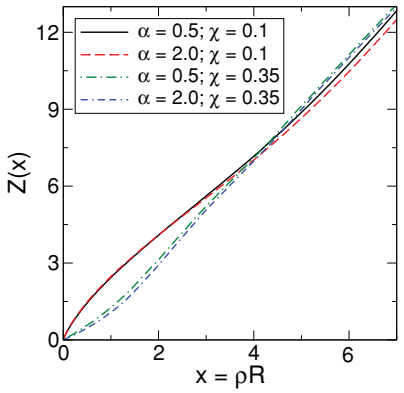

FIG. 11. (Color online) Cumulative coordination numbers $Z(R)$ for numerically constructed hyperuniform point patterns with small-wavenumber exponents $\alpha = 0.5$ and $\alpha = 2.0$. The fractions of constrained degrees of freedom are $\chi = 0.1$ and $\chi = 0.35$.

enforce hyperuniformity of the point pattern by overcoming the highly inhomogeneous local structure of the clusters. In the context of our analysis above, for small perturbations from the ideal gas, the high configurational degeneracy that remains after constraining only a few degrees of freedom implies that highly disordered configurations are most likely to appear from our numerical constructions. However, with the added implicit constraint of hyperuniformity the system will sacrifice local structural regularity for clustering of points that are globally separated by sufficiently large voids, resulting in a negatively correlated exclusion correlation function.

Figure 11 highlights this behavior by examining the cumulative coordination numbers $Z(R)$ at $\chi = 0.1$ and $\chi = 0.35$ for our systems. Although at $\chi = 0.1$ the $\alpha = 2$ system exhibits greater clustering at small-r than for $\alpha = 0.5$, at large r this trend reverses, which is consistent with the appearance of larger voids with higher probability and supports our claim that these voids serve to regularize the global structures of the systems. Using the lower bound (55) on the particle exclusion probability function, we also observe explicitly the effect of the locally clustered structure on the small-r particle exclusion probability.

On reaching $\chi = 0.35$, we recover the usual behavior associated with hyperuniformity. By constraining a sufficient number of degrees of freedom, the effective interparticle repulsions induced by the collective coordinate constraints control the small-r region of the pair correlation function (and, therefore, the cumulative coordination number), prohibiting local cluster formation. The regularizing factor in this case is therefore the distribution of voids within the particle space, contained in $E_P(r)$. Indeed, the void exclusion probability $E_V(r)$ is highly constrained by this effective repulsion and decays to zero faster than $E_P(r)$, resulting in a positively correlated exclusion correlation function. By increasing the exponent α governing the small-wavenumber region of the structure factor, we observe increased regularity in the local structure, corresponding to a decreased $Z(R)$ and $E_V(r)$ and a particle exclusion correlation function $E_P(r)$ that decays more rapidly to zero, in perfect accordance with the aforementioned void-space criterion on hyperuniformity put forth by Gabrielli and Torquato [43]. It is also noteworthy that increased void-space constraints associated with increased α are consistent with the behavior of the structure factor for MRJ hard-sphere packings, about which we have more to say in Sec. VI.

VI. CONCLUDING REMARKS AND DISCUSSION

We have provided the first known constructions of disordered hyperuniform many-particle ground states possessing anomalous local density fluctuations induced by a sublinear small-wavenumber scaling in the structure factor. Such systems are defined by a number variance $\sigma_N^2(R)$ that asymptotically scales faster than the surface area of an observation window but slower than the window volume. By controlling the collective density variables associated with the underlying point pattern, we have also been able to probe the relationship between interparticle correlations and constraints on the local coordination structure. Specifically, we have provided detailed statistics to measure the distribution of the *void space* external to the particles, including measurements of the void and particle exclusion probabilities.

Under sufficiently low constraints on the system, our numerically constructed disordered many-particle ground states exhibit substantial clustering, resulting in a highly inhomogeneous local structure. However, on the global scale of the system as measured by asymptotic local density fluctuations, these local clusters are separated by comparatively large interparticle voids, thereby regularizing the microstructure and preserving the constraint of hyperuniformity that we impose. Indeed, this effect becomes more pronounced on passing from the "anomalous" regime of hyperuniformity to the more usual case, where $\sigma_N^2(R) \sim R^{d-1}$ asymptotically (i.e., for all periodic point patterns, quasicrystals with Bragg peaks, and disordered systems with pair correlations decaying exponentially fast) [4,6]. On increasing the fraction of constrained degrees of freedom within the system, we are able to preclude this clustering affect by reinforcing the effective interparticle repulsion imposed by our targeted structure factor $S(k)$. Furthermore, we have shown that this effective repulsion becomes increasingly more pronounced as the exponent α governing the small-wavenumber scaling of $S(k)$ is increased.

It follows from these observations that one can formally define an effective repulsive radius around each point within a hyperuniform point pattern. However, so long as this radius is not substantially large compared to the expected interparticle spacing $\rho^{-1/d}$, i.e., in the absence of microstructural constraints, clustering effects can still dominate the interparticle correlations and the local coordination structure. We have shown that this effect is entropically favorable since slight deviations from the ideal gas are still associated with an exponentially large configurational degeneracy. However, this degeneracy is expected to increase rapidly on constraining a sufficient number of degrees of freedom or, equivalently, increasing the effective repulsive radius. We have shown that this loss of configurational degeneracy is associated with a highly constrained void space distribution, which can be considered as a signature of predominantly "repulsive" hyperuniform point patterns.

Our results have particular implications for understanding the appearance and nature of hyperuniformity in MRJ packings of hard spheres. It is interesting to note that equilibrium

distributions of hard spheres are known not to be hyperuniform [4] except at the close-packed density, at which point the system freezes into a crystal with long-range order. MRJ hard-sphere packings are therefore unique in that they are *nonequilibrium* systems that are uniformly mechanically rigid, and it is this rigidity that has been shown to be essential for the onset of hyperuniformity (with logarithmic asymptotic local density fluctuations) [13]. Importantly, rigidity places severe geometric constraints on the local arrangements of particles [45] and has been shown to regularize the void space distribution on the global scale of the microstructure [13]. We have demonstrated in this work that by decreasing the exponential form of the structure factor within the small-wavenumber region, these void-space constraints are relaxed in accordance with the decreased effective radius surrounding the particles. Since MRJ packings are *maximally* disordered among all strictly jammed packings, it follows that such systems must already possess the maximal number of degrees of freedom consistent with the geometric constraints of strict jamming. Therefore, *any* increase in the distribution of the void sizes is inconsistent with these same constraints, highlighting why exponents $\alpha < 1$ in the small-wavenumber scaling of $S(k)$ have never been observed for such systems.

Our work has also raised a number of interesting questions related to the physics of collective coordinate constraints. These issues are especially important since the construction of hyperuniform systems via collective coordinate constraints has played a fundamental role in the development of "stealth" materials transparent to radiation of certain frequencies [11], the identification of unusual classical disordered ground states [22], and the design of novel disordered materials with complete photonic band gaps [10]. The mathematical properties associated with collective coordinates are surprisingly subtle and have only partially been explored in the literature [20,21]. Constraining a collective density variable, including, for example, either a complete suppression to zero or fixing its magnitude, results in a highly nonlinear equation relating the components of the particle positions $\{\mathbf{r}_j\}$. For higher-dimensional systems, it has been previously observed [22] that these nonlinear equations have a tendency to "couple" in such a way that one must go beyond $\chi = 0.5$ to crystallize the system, meaning that one cannot simply count constraints and degrees of freedom. The analytical techniques available for one-dimensional systems [20], therefore, do not easily extend to higher dimensions. It is an open problem to determine analytically the relationship between χ and the "true" number of constrained degrees of freedom; recent work has examined the fraction of normal modes with vanishing frequency as a more appropriate indicator of the latter [22]. We have provided some analysis here in one dimension to suggest how the configuration space is constrained with increasing χ by determining the entropy for small deviations from the ideal gas. Certainly for higher values of χ our simple linear scaling will break down; characterizing the deviations from this linear behavior, especially in higher dimensions, is an attractive problem warranting further consideration.

ACKNOWLEDGMENTS

This research was supported by the US Department of Energy, Office of Basic Energy Sciences, Division of Materials Sciences and Engineering under Award DE-FG02-04-ER46108.

APPENDIX: MATHEMATICAL RELATIONSHIP BETWEEN THE VOID AND PARTICLE EXCLUSION PROBABILITY FUNCTIONS

One can relate the void and particle exclusion probabilities via a simple probabilistic construction [15]. Specifically, we consider a generalized exclusion probability $E_V(r;\epsilon)$, which is the probability of finding a d-dimensional annulus of outer radius r and inner radius ϵ; by definition, $E_V(r;0) = E_V(r)$. Taking the derivative of this function with respect to the inner radius ϵ gives a function proportional to the probability of finding a point within a small radial region inside the annulus and the annulus itself devoid of points. It follows that $E_P(r)$, the conditional probability of finding a spherical cavity centered on a point, is

$$E_P(r) = \lim_{\epsilon \to 0^+} \frac{1}{\rho s(\epsilon)} \frac{\partial E_V(r;\epsilon)}{\partial \epsilon}, \tag{A1}$$

where $s(\epsilon)$ is the surface area of a d-dimensional sphere of radius ϵ. This construction is known in the theory of point processes [46] and has also been used in the literature to identify the void statistics of certain point patterns related to problems in number theory, random matrix theory, and quantum mechanics [14].

[1] We adopt the term *regularity* here as opposed to *homogeneity* in order to characterize the extent of global order of a structure since the latter term has a highly specialized meaning in the statistical sciences.

[2] D. Chandler, *Introduction to Modern Statistical Mechanics* (Oxford University Press, New York, 1987).

[3] A *Bravais lattice* in d-dimensional Euclidean space $\mathbb{R}^d$ is a periodic point pattern formed by taking integral linear combinations of d basis vectors; it has exactly one particle per fundamental cell. More generally, one can also define periodic non-Bravais lattices, or lattices with a multiparticle basis, by taking the union of a Bravais lattices with N of its translates, resulting in $N+1$ particles per fundamental cell.

[4] S. Torquato and F. H. Stillinger, Phys. Rev. E **68**, 041113 (2003).

[5] S. Torquato, T. M. Truskett, and P. G. Debenedetti, Phys. Rev. Lett. **84**, 2064 (2000).

[6] C. E. Zachary and S. Torquato, J. Stat. Mech.: Theory and Expt. (2009) P12015.

[7] P. J. Steinhardt, D. R. Nelson, and M. Ronchetti, Phys. Rev. B **28**, 784 (1983).

[8] S. Torquato and F. H. Stillinger, Rev. Mod. Phys. **82**, 2633 (2010).

[9] L. Pietronero, A. Gabrielli, and F. S. Labini, Physica A **306**, 395 (2002).

[10] M. Florescu, S. Torquato, and P. J. Steinhardt, Proc. Nat. Acad. Sci. USA **106**, 20658 (2009); Phys. Rev. B **80**, 155112 (2009).

[11] R. D. Batten, F. H. Stillinger, and S. Torquato, J. Appl. Phys. **104**, 033504 (2008). A *stealth material* in this context refers to a many-particle configuration that completely suppresses scattering of incident radiation for a set of wave vectors, and, thus, is transparent at these wavelengths.
[12] A. Donev, F. H. Stillinger, and S. Torquato, Phys. Rev. Lett. **95**, 090604 (2005).
[13] C. E. Zachary, Y. Jiao, and S. Torquato, Phys. Rev. Lett. **106**, 178001 (2011); Phys. Rev. E **83**, 051308 (2011); **83**, 051309 (2011).
[14] S. Torquato, A. Scardicchio, and C. E. Zachary, J. Stat. Mech.: Theory and Expt. (**2008**) P11019.
[15] A. Scardicchio, C. E. Zachary, and S. Torquato, Phys. Rev. E **79**, 041108 (2009).
[16] L. Reatto and G. V. Chester, Phys. Rev. **155**, 88 (1967).
[17] P. J. E. Peebles, *Principles of Physical Cosmology* (Princeton University Press, Princeton, NJ, 1998).
[18] O. U. Uche, S. Torquato, and F. H. Stillinger, Phys. Rev. E **74**, 031104 (2006).
[19] A. Gabrielli, M. Joyce, and S. Torquato, Phys. Rev. E **77**, 031125 (2008).
[20] Y. Fan, J. K. Percus, D. K. Stillinger, and F. H. Stillinger, Phys. Rev. A **44**, 2394 (1991).
[21] O. U. Uche, F. H. Stillinger, and S. Torquato, Phys. Rev. E **70**, 046122 (2004).
[22] R. D. Batten, F. H. Stillinger, and S. Torquato, Phys. Rev. Lett. **103**, 050602 (2009); Phys. Rev. E **80**, 031105 (2009).
[23] S. Torquato and F. H. Stillinger, Phys. Rev. Lett. **100**, 020602 (2008); S. Torquato, C. E. Zachary, and F. H. Stillinger, Soft Matter **7**, 3780 (2011).
[24] W. Man, M. Florescu, K. Matsuyama, P. Yadak, S. Torquato, and P. J. Steinhardt, *Conference on Lasers and Electro-Optics* (Optical Society of America, Washington, DC, 2010).
[25] J.-P. Hansen and I. R. McDonald, *Theory of Simple Liquids*, 3rd ed. (Elsevier, London, 2006).
[26] Equation (18) should rigorously be interpreted in the thermodynamic limit since the $\mathbf{k} = \mathbf{0}$ mode contains an $\mathcal{O}(1/N)$ correction to the long-range behavior of g_2.
[27] J. de Coninck, F. Dunlop, and T. Huillet, Physica A **387**, 725 (2008). Examples where the number variance grows faster than the window volume have been observed in the literature and are related to thermodynamic critical points.
[28] J. E. Dennis and H. W. Mei, J. Optim. Theory Appl. **28**, 455 (1979).
[29] L. Kaufman, SIAM J. Optim. **10**, 56 (1999).
[30] *Mathematical Physics in One Dimension*, edited E. H. Lieb and D. C. Mattis (Academic Press, New York, 1966).
[31] For the one-dimensional case where $S_0(k) = 0$ for all $k \in \mathcal{Q}$, $\chi = 1/2$ as defined in (30) corresponds to a loss of all degrees of freedom. To see this, note that $S_0(k) = 0$ is equivalent to requiring $\hat{\rho}(k) = 0$, which places two independent constraints, corresponding to real and imaginary parts, on the N degrees of freedom [20].
[32] For reasons that we discuss in Sec. VI, in higher dimensions one cannot simply use the number of vanishing collective coordinates to predict the value of χ at which the disorder order phase transition occurs. Numerical work in the literature suggests that the threshold values of χ in two and three dimensions are, respectively, 0.77990 and 0.50066 [11,18].
[33] The case $S_0(\mathbf{k}) = 0$ can be recovered either as the limit $\alpha \to +\infty$ or by taking $D = 0$.
[34] S. Torquato and F. H. Stillinger, J. Phys. Chem. B **106**, 8354 (2002); Expt. Math. **15**, 307 (2006).
[35] A. J. Coleman, Rev. Mod. Phys. **35**, 668 (1963).
[36] M. Yamada, Prog. Theor. Phys. **25**, 579 (1961).
[37] T. Kuna, J. L. Lebowitz, and E. R. Speer, J. Stat. Phys. **129**, 417 (2007).
[38] Y. Jiao, F. H. Stillinger, and S. Torquato, Phys. Rev. E **81**, 011105 (2010).
[39] S. Torquato, B. Lu, and J. Rubinstein, J. Phys. A: Math. Gen. **23**, L103 (1990); Phys. Rev. A **41**, 2059 (1990).
[40] S. Torquato, *Random Heterogeneous Materials: Microstructure and Macroscopic Properties* (Springer, New York, 2002).
[41] S. Torquato, Phys. Rev. E **82**, 056109 (2010).
[42] S. Torquato, J. Stat. Phys. **45**, 843 (1986).
[43] A. Gabrielli and S. Torquato, Phys. Rev. E **70**, 041105 (2004).
[44] L. Pauling, J. Am. Chem. Soc. **57**, 2680 (1935); J. Snyder, J. S. Slusky, R. J. Cava, and P. Schiffer, Nature **413**, 48 (2001); S. V. Isakov, R. Moessner, S. L. Sondhi, Phys. Rev. Lett. **95**, 217201 (2005); C. H. Henley, Annu. Rev. Condens. Matter Phys. **1**, 179 (2010). Note that the analog of the hyperuniformity concept in spin systems is when they possess zero net magnetization on large length scales.
[45] A. Donev, S. Torquato, and F. H. Stillinger, J. Comput. Phys. **202**, 737 (2005).
[46] D. J. Daley and D. Vere-Jones, *An Introduction to the Theory of Point Processes: Elementary Theory and Methods*, 2nd ed. (Springer, New York, 2008), Vol. I.